

# Synthetic 1,4-anthracenedione analogs induce cytochrome *c* release, caspase-9, -3, and -8 activities, poly(ADP-ribose) polymerase-1 cleavage and internucleosomal DNA fragmentation in HL-60 cells by a mechanism which involves caspase-2 activation but not Fas signaling

Elisabeth M. Perchellet<sup>a</sup>, Yang Wang<sup>a</sup>, Rebeka L. Weber<sup>a</sup>, Bonnie J. Sperfslage<sup>a</sup>, Kaiyan Lou<sup>b</sup>, Justin Crossland<sup>b</sup>, Duy H. Hua<sup>b</sup>, Jean-Pierre Perchellet<sup>a,\*</sup>

<sup>a</sup>Anti-Cancer Drug Laboratory, Division of Biology, Ackert Hall, Kansas State University, Manhattan, KS 66506-4901, USA

<sup>b</sup>Department of Chemistry, Kansas State University, Manhattan, KS 66506-4901, USA

Received 5 May 2003; accepted 16 September 2003

## Abstract

Synthetic analogs of 1,4-anthraquinone (AQ code number), a compound that mimics the antiproliferative effects of daunorubicin (daunomycin) in the nanomolar range *in vitro* but has the advantage of blocking nucleoside transport and retaining its efficacy in multidrug-resistant tumor cells, were tested for their ability to induce apoptosis in the HL-60 cell system. AQ10 and, especially, the new lead antiproliferative compounds AQ8 and AQ9 reduce the growth and integrity of wild-type, drug-sensitive, HL-60-S cells more effectively than AQ1, suggesting that various methyl group substituents at C6 may enhance the bioactivity of the parent compound. Internucleosomal DNA fragmentation, a late marker of apoptosis, is similarly induced in a biphasic manner by increasing concentrations of AQ8 and AQ9 at 24 hr. Poly(ADP-ribose) polymerase-1 (PARP-1) cleavage, an early event required for cells committed to apoptosis, is detected within 3–6 hr in HL-60-S cells treated with AQ9. In accord with the fact that the caspases 9 and 3 cascade is responsible for PARP-1 cleavage, the activities of initiator caspase-9 and effector caspase-3 are induced by AQ9 in the same time- and concentration-dependent manners and to the same maximal degrees in both the HL-60-S and multidrug-resistant HL-60-RV cell lines. Interestingly, a 1-hr pulse treatment is sufficient for AQ8 and AQ9 to maximally induce caspase-9 and -3 activities at 6 hr. The release of mitochondrial cytochrome *c* (Cyt *c*) is also detected within 3–6 hr in HL-60-S cells treated with AQ9, a finding consistent with the fact that Cyt *c* is the apoptotic trigger that activates caspase-9. Moreover, AQ analogs induce Cyt *c* release, caspase-9 and -3 activities and PARP-1 cleavage in relation with their abilities to decrease tumor cell growth and integrity, AQ8 and AQ9 being consistently the most effective. Since apical caspases 2 and 8 may both act upstream of mitochondria to promote Cyt *c* release, it is significant to show that AQ9 maximally induces caspase-2 and -8 activities at 6 and 9 hr, respectively. During AQ8 treatment, the caspase-2 inhibitor benzyloxycarbonyl (z)-Val-Asp-Val-Ala-Asp (VDVAD)-fluoromethyl ketone (fmk) totally blocks caspase-9, -3, and -8 activations, whereas the caspase-8 inhibitor z-Ile-Glu-Thr-Asp-(IETD)-fmk does not prevent caspase-2, -9, and -3 activations, suggesting that AQ-induced caspase-2 activity is an upstream event critical for the activation of the downstream caspases 9 and 3 cascade, including the mitochondrial amplification loop through caspase-8. However, these caspase-2 and -8 inhibitors fail to alter AQ8-induced Cyt *c* release, suggesting that AQs might also target mitochondria independently from caspase activation. Furthermore, the antagonistic anti-Fas DX2 and ZB4 monoclonal antibodies (mAbs), which block the induction of Cyt *c* release and caspase-2, -8, and -9 activities by the agonistic anti-Fas CH11 mAb, and the neutralizing anti-Fas ligand (FasL) NOK-1 mAb all fail to inhibit AQ9-induced Cyt *c* release and caspase-2, -8, and -9 activities,

\* Corresponding author. Tel.: +1-785-532-7727; fax: +1-785-532-6653.

E-mail address: [jpperch@ksu.edu](mailto:jpperch@ksu.edu) (J.-P. Perchellet).

**Abbreviations:** Ac-LEHD, acetyl-Leu-Glu-His-Asp; AFC, 7-amino-4-trifluoromethylcoumarin; AIF, apoptosis-inducing factor; Apaf-1, apoptotic protease-activating factor-1; AQ, anthraquinone (anthracenedione); Cyt *c*, cytochrome *c*; DAU, daunorubicin (daunomycin); DEVD, Asp-Glu-Val-Asp; DOX, doxorubicin (adriamycin); FasL, Fas ligand; fmk, fluoromethyl ketone; FCS, fetal bovine calf serum; IAP, inhibitor of apoptosis; IETD, Ile-Glu-Thr-Asp; mAb, monoclonal antibody; MDR, multidrug-resistant(t)ce; MPT, mitochondrial permeability transition; MTS, 3-(4,5-dimethylthiazol-2-yl)-5-(3-carboxymethoxyphenyl)-2-(4-sulfophenyl)-2H-tetrazolium; PARP-1, poly(ADP-ribose) polymerase-1; PBS, Ca<sup>2+</sup>/Mg<sup>2+</sup>-free Dulbecco's phosphate-buffered saline; P-gp, P-glycoprotein; PMS, phenazine methosulfate; PMSF, phenylmethylsulfonyl fluoride; SAR, structure–activity relationship; tBid, truncated Bid; Topo, DNA topoisomerase; VDVAD, Val-Asp-Val-Ala-Asp; WT, wild-type; z, benzyloxycarbonyl.

suggesting that the FasL/Fas signaling pathway is not involved in the mechanism by which antiproliferative AQ analogs trigger apoptosis in HL-60 cells.

© 2003 Elsevier Inc. All rights reserved.

**Keywords:** 1,4-Anthracenediones; Apoptosis; Fas; Cytochrome *c*; Caspases; Poly(ADP-ribose) polymerase-1; DNA fragmentation; HL-60 cells

## 1. Introduction

Although the exact bioactivity of their quinoid ring remains unclear, quinone antitumor drugs, such as doxorubicin (adriamycin, DOX) and daunorubicin (daunomycin, DAU), may be cytotoxic because of their involvement in soft electrophilic arylation and redox cycling oxidation [1–4]. DOX and DAU covalently bind to and intercalate into DNA, inhibit DNA replication and RNA transcription, are DNA topoisomerase (Topo) II poisons, produce oxidative stress and damage biomembranes, induce DNA breakage and chromosomal aberrations, and have a wide spectrum of anticancer activity [2–7]. Since the clinical effectiveness of DOX and DAU is severely limited by their cumulative cardiotoxicity and ability to induce multidrug-resistance (MDR), it is important to develop new quinone antitumor drugs with improved bioactivity [2].

Recently, we discovered that, in contrast to its inactive precursor quinizarin (1,4-dihydroxy-9,10-anthraquinone; AQ2), anthracene-1,4-dione (1,4-anthraquinone; AQ1) is cytostatic ( $IC_{50}$ : 9 nM based on cell number and 25 nM based on mitochondrial metabolism) in the same nanomolar range as DAU in the L1210 leukemic cell system *in vitro* [8]. AQ1 and, to a lesser degree, its derivative 6,7-dichloro-1,4-anthracenedione (AQ4) mimic all the effects of DAU tested so far in leukemic cells *in vitro* [8,9]. They decrease L1210 and HL-60-S tumor cell proliferation within 2–4 days and inhibit DNA, RNA, and protein syntheses within 2–3 hr. They reduce the mitotic index within 24 hr, suggesting that they arrest earlier stages of cell cycle progression to prevent tumor cells from accumulating in M-phase. Moreover, AQ1 induces as much DNA cleavage at 24 hr as camptothecin and DAU, two anticancer drugs producing DNA strand breaks and known to inhibit Topo I and II activities, respectively. But the critical finding is that AQ1 has the additional advantage of blocking the cellular transport of purine and pyrimidine nucleosides within 15 min, an effect which DAU cannot do [8,9]. The effects of AQ1 persist upon drug removal, suggesting that this compound may rapidly interact with various molecular targets in cell membranes and nuclei to trigger irreversible or, at least, long-lasting events which disrupt the function of nucleoside transporters and nucleic acids after cessation of drug treatment. In addition to their potency and unusual mechanism of action, AQ1 and AQ4 retain their efficacy in two MDR HL-60 sublines that have already developed different P-glycoprotein (P-gp)- and MDR-associated protein-mediated mechanisms of resistance to DAU, suggesting that these new quinone antiproliferative drugs might

have other molecular targets than those of DAU and might be valuable in polychemotherapy to potentiate the action of antimetabolites and circumvent MDR [8,9].

Many anticancer drugs, such as DOX and DAU, may activate apoptosis at low concentrations to kill susceptible tumor cells while defective apoptotic signaling pathways may contribute to the development of MDR [6,7,10–16]. Drug-damaged tumor cells irreversibly committed to the apoptotic pathway exhibit characteristic biochemical and morphological alterations, including mitochondrial dysfunction, cytoplasmic and nuclear condensation, plasma membrane blebbing, DNA degradation into oligonucleosomal fragments, and packaging of cellular components into discrete membrane-bound apoptotic bodies that are rapidly phagocytosed by surrounding cells and macrophages [17]. Whether death receptor dependent or independent, the different apoptosis signaling pathways induced by various anticancer drugs with distinct primary subcellular targets and mechanisms of actions may converge on mitochondria to cause permeability transition (MPT), release apoptogenic factors, and activate a similar caspase proteolytic cascade that is amplified by a positive feedback loop involving the release of Cyt *c* from mitochondria [12,18,19].

Since apoptosis is an active ATP-driven and cell cycle phase-specific process that requires the expression of specific genes, the synthesis of new RNA and proteins and the activation of caspases, non-caspase proteases and nucleases, inhibitors of such mechanisms can prevent DNA fragmentation in anthracycline-treated cells (reviewed in Ref. [6]). Interestingly, the concentration-dependent inductions of DNA cleavage by AQ1 and DAU in L1210 and HL-60-S cells at 24 hr are similarly biphasic, suggesting that, even though they are increasingly cytostatic, higher concentrations of AQ1 and DAU inhibit RNA and protein syntheses to such excessive degrees that they abolish their own ability to sustain the active process of apoptotic DNA fragmentation induced by low concentrations of these compounds [8,9]. Indeed, the optimal concentrations of 1.6  $\mu$ M DAU and 4  $\mu$ M AQ1, which normally induce peak levels of DNA fragmentation in L1210 cells at 24 hr, similarly lose their ability to do so in the presence of actinomycin D, cycloheximide, and aurointricarboxylic acid, suggesting that new RNA and protein synthesis and the activation of endonuclease enzymes are all involved in the mechanisms by which these quinone drugs induce apoptotic DNA fragmentation [8].

Because neoplastic cells undergoing apoptosis may be phagocytosed without inflammation, lead antiproliferative

AQ1 analogs that are the most effective compounds in the series and can induce apoptosis may be valuable to develop new means of polychemotherapy. Hence, the present study was undertaken to identify more potent AQ1 analogs and to characterize the sequential markers of apoptosis that are involved in the molecular mechanism by which they induce internucleosomal DNA fragmentation. Two substantially more cytostatic AQ1 analogs have been synthesized and demonstrated to induce Cyt *c* release, caspase-9, -3, and -8 activation, PARP-1 cleavage, and internucleosomal DNA fragmentation by a caspase-2-mediated and Fas-independent signaling pathway in wild-type (WT) and MDR HL-60 cells.

## 2. Materials and methods

### 2.1. Cell cultures and drug treatments

The synthesis of AQ1 has been reported (reviewed in Ref. [8]). All solutions of synthetic AQ1 analogs, z-VDVAD-fmk and z-IETD-fmk (both from Calbiochem) were dissolved and diluted in DMSO, whereas solutions of anti-Fas DX2, anti-FasL NOK-1 (both from BD Pharmin-gen), anti-Fas CH11, and anti-Fas ZB4 (both from Upstate Biotechnology) mAbs were formulated in  $\text{Ca}^{2+}/\text{Mg}^{2+}$ -free Dulbecco's phosphate-buffered saline (PBS). Suspension cultures of WT, drug-sensitive, human HL-60-S promyelocytic leukemia cells (American Type Culture Collection) were maintained in continuous exponential growth by twice-a-week passage in RPMI 1640 medium supplemented with 8.25% fetal bovine calf serum (FCS; Atlanta Biologicals) and penicillin (100 IU/mL)–streptomycin (100  $\mu\text{g}/\text{mL}$ ) and incubated in the presence or absence (control) of drugs at 37° in a humidified atmosphere containing 5%  $\text{CO}_2$  [9]. The MDR HL-60-RV cells shown to overexpress P-gp were similarly maintained in RPMI 1640 medium in the absence of drugs but were exposed, every 4 weeks, to 41 nM DAU for 48 hr to stabilize their MDR phenotype [9,20]. This concentration of DAU, which is not cytotoxic to MDR HL-60 cells, was removed from the culture medium at least 48 hr before experimentation. Since drugs were supplemented to the culture medium in 1-, 6-, or 10- $\mu\text{L}$  aliquots, the concentration of vehicle (0.2% DMSO) in the final incubation volumes (0.5, 3, or 5 mL, respectively) did not interfere with the data [9,21]. For 1-hr pulse treatment in the caspase experiments, drug-containing supernatants were discarded after centrifugation at 200 *g* for 10 min, and tumor cells were washed with, and resuspended in, fresh RPMI 1640 medium for further incubation [8,21].

### 2.2. Cell proliferation and integrity assays

The growth of drug-treated WT HL-60-S cells (initial density  $3.75 \times 10^4$  cells/0.5 mL) was assessed from their

mitochondrial ability to bioreduce the 3-(4,5-dimethylthiazol-2-yl)-5-(3-carboxymethoxyphenyl)-2-(4-sulfophenyl)-2*H*-tetrazolium (MTS) reagent (Promega) in the presence of phenazine methosulfate (PMS; Sigma) into a water-soluble formazan product which absorbs at 490 nm [22]. After 4 days at 37° in 48-well Costar culture plates, control and drug-treated cell samples (about  $10^6/0.5$  mL/well for controls) were further incubated at 37° for 3 hr in the dark in the presence of 0.1 mL of MTS:PMS (2:0.1) reagent and their relative metabolic activity was estimated by recording the absorbance at 490 nm, using a Cambridge model 750 automatic microplate reader (Packard). Blank values for culture medium supplemented with MTS:PMS reagent in the absence of cells were subtracted from the results [8,9]. Drug effectiveness against leukemic cells was confirmed using the Trypan blue exclusion test [23,24]. After HL-60-S cells ( $0.5 \times 10^6/\text{mL}$ ) were incubated for 24 hr in the presence or absence of AQ1 analogs, the numbers of cells with intact (unstained) and disrupted plasma membrane (stained) were counted within 5–7 min of 0.2% Trypan blue addition. The loss of cellular integrity (% stained cells) assessed by this dye exclusion technique is consistent with the degree of apoptosis observed in HL-60 cells treated with cytotoxic drugs [23,24].

### 2.3. Detection of DNA fragmentation

Drug-induced DNA cleavage was determined by intact chromatin precipitation, using WT HL-60-S cells which were prelabeled with 1  $\mu\text{Ci}$  [*methyl*- $^3\text{H}$ ]thymidine (50 Ci/mmol; Amersham) for 2 hr at 37°, washed with  $3 \times 1$  mL of ice-cold PBS, collected by centrifugation, resuspended in fresh medium at a density of  $5 \times 10^5$  cells/0.5 mL, and then incubated at 37° for 24 hr in the presence or absence (control) of drugs [8,9]. After centrifugation at 200 *g* for 10 min to discard the drugs and wash the cells, the cell pellets were lysed for 20 min in 0.5 mL of ice-cold hypotonic lysis buffer containing 10 mM Tris-HCl, pH 8.0, 1 mM EDTA, and 0.2% Triton X-100, and centrifuged at 12,000 *g* for 15 min to collect the supernatants. The radioactivity in the supernatants (detergent-soluble low molecular weight DNA fragments) and the pellets (intact chromatin DNA) was determined by liquid scintillation counting: % DNA fragmentation =  $[\text{cpm in supernatant} / \text{cpm in supernatant} + \text{pellet}] \times 100$  [6,8,9,25,26]. Before being counted in 6 mL of Bio-Safe NA (Research Products International), the intact pelleted chromatin was incubated for 2 hr at 60° in the presence of 0.6 mL of NCS tissue solubilizer (Amersham) [9,25,26]. For internucleosomal DNA fragmentation, HL-60-S cells were incubated at 37° for 24 hr in the presence or absence (control) of drugs and DNA was extracted from samples with equal cell densities ( $10^6$  cells/0.5 mL), using a salting out procedure [26–28]. Cell pellets were washed twice with PBS, lysed overnight at 37° in 0.34 mL of 10 mM Tris-HCl, pH 8.0, containing 2 mM EDTA, 400 mM NaCl, 1% SDS, and proteinase K

(0.5 mg/mL), vortexed for 15 s with 0.1 mL of 6 M NaCl and centrifuged ( $2500\text{ g} \times 30\text{ min}$ ), and DNA was precipitated from the supernatants (0.44 mL) with 0.88 mL of 100% EtOH for 15 min at  $4^{\circ}$ . After centrifugation ( $14,000\text{ g} \times 15\text{ min}$ ) at  $4^{\circ}$ , the air-dried DNA pellets were dissolved in 0.34 mL of 10 mM Tris–HCl, pH 8.0, with 1 mM EDTA (TE buffer) and incubated for 2 hr at  $37^{\circ}$  in the presence of RNase (0.1 mg/mL). After another round of EtOH precipitation and centrifugation, the final air-dried pellets were dissolved in 50  $\mu\text{L}$  of TE buffer and their DNA concentrations determined spectrophotometrically at 260 nm. Equal amounts of DNA samples (6  $\mu\text{g}/7.5\text{ }\mu\text{L}$  TE buffer) were mixed with 1.5  $\mu\text{L}$  of 10 mM Tris–HCl, pH 7.5, containing 50 mM EDTA, 10% Ficoll 400, and 0.4% Orange G, and loaded on each lane. About 0.5  $\mu\text{g}$  of 100 bp DNA ladder and 0.75  $\mu\text{g}$  of lambda DNA/*EcoRI* + *HindIII* (both from Promega) were similarly applied to each gel to provide size markers in the range 100–1500 and 125–21,226 bp, respectively. Horizontal electrophoresis of DNA samples was performed for 3.7 hr at 60 V in 1.5% agarose gels containing ethidium bromide (1  $\mu\text{g}/\text{mL}$ ) with 90 mM Tris–HCl, pH 8.0, containing 90 mM boric acid and 2 mM EDTA as a running buffer. DNA fragments were visualized and photographed with Polaroid 667 film under UV light at 312 nm, using a FisherBiotech model 88A variable-intensity UV transilluminator [26,28].

#### 2.4. Fluorogenic assay of caspase activities

Control and drug-treated HL-60-S or HL-60-RV cells ( $0.4 \times 10^6/0.5\text{ mL}$ ) were incubated in triplicate for various periods of time at  $37^{\circ}$ , collected by centrifugation at 200 g for 10 min, and washed with 1 mL of ice-cold PBS. Cell pellets were resuspended in chilled 10 mM HEPES buffer, pH 7.4, containing 100 mM NaCl, 100 mM KCl, 5 mM  $\text{MgCl}_2$ , 1 mM EDTA, 10 mM EGTA, 10% sucrose, 1 mM phenylmethylsulfonyl fluoride (PMSF), 1 mM DTT, and 100  $\mu\text{M}$  digitonin (175  $\mu\text{L}$  for caspase-3 assay and 120  $\mu\text{L}$  for caspase-2, -8, and -9 assays), and lysed for 10 min on ice. Cell lysates were centrifuged at  $14,000\text{ g}$  for 20 min at  $4^{\circ}$  to precipitate cellular debris and the supernatants were stored frozen at  $-70^{\circ}$  overnight. The caspases 2-, 3-, 8-, and 9-like activities of the lysates were determined in reaction mixtures that contained 50  $\mu\text{L}$  of lysis buffer (blank) or supernatant (control or drug-treated samples) and 50  $\mu\text{L}$  of reaction buffer (100 mM HEPES, pH 7.5, containing 1 mM EDTA, 10 mM EGTA, 10% sucrose, and 10 mM of freshly prepared DTT) and that were initiated by the addition of 5- $\mu\text{L}$  aliquots of the respective 5 mM z-VDVAD-7-amino-4-trifluoromethylcoumarin (AFC), 1 mM z-Asp-Glu-Val-Asp (DEVD)-AFC, 1 mM z-IETD-AFC or 5 mM acetyl-Leu-Glu-His-Asp (Ac-LEHD)-AFC stocks of AFC–substrate conjugates (all from Calbiochem). After incubation for 1 hr at  $37^{\circ}$  in 96-well Costar white polystyrene assay plates, the fluorescence of the free AFC released upon proteolytic cleavage of the substrate by

the appropriate caspase was detected at 400 nm excitation and 505 nm emission, using a Cary Eclipse Fluorescence Spectrophotometer equipped with microplate reader accessory (Varian). Arbitrary fluorescence units were quantified with reference to calibration curves ranging from 0.01 to 6 nmol AFC (from Sigma), the protein concentrations of the supernatants were determined using the BCA Protein Assay Kit (Pierce), and the VDVAD-, DEVD-, IETD-, and LEHD-specific cleavage activities of the samples were expressed as nanomoles of AFC released/milligram of protein. Data of all biochemical experiments were analyzed using Student's *t* test with the level of significance set at  $P < 0.05$ .

#### 2.5. Western blot analysis of PARP-1 cleavage and Cyt *c* release

Suspensions of control and drug-treated HL-60-S cells (initial density  $1.3 \times 10^6\text{ cells/mL}$ ) were incubated for various periods of time at  $37^{\circ}$  in 15 mm  $\times$  60 mm Petri dishes containing final volumes of 3 or 5 mL for PARP-1 or Cyt *c* analysis, respectively. For PARP-1 cleavage,  $3.9 \times 10^6$  tumor cells were collected by centrifugation, washed with 1 mL of PBS, lysed with 40  $\mu\text{L}$  of 50 mM Tris–HCl buffer, pH 7.4, containing 250 mM NaCl, 1 mM  $\text{CaCl}_2$ , 50 mM NaF, 0.1% Triton X-100, and protease inhibitors (0.2 mg leupeptin/mL, 0.2 mg aprotinin/mL, 10 mg PMSF/mL), and disrupted by sonication with microtip for 15 strokes at power level 4, using a 250 W Vibra Cell Ultrasonic Processor (Sonics & Materials) [21]. For Cyt *c* release, pellets of  $6.5 \times 10^6$  PBS-washed cells were lysed for 30 min on ice with 80  $\mu\text{L}$  of 10 mM HEPES buffer, pH 7.4, containing 100 mM NaCl, 100 mM KCl, 5 mM  $\text{MgCl}_2$ , 1 mM EDTA, 10 mM EGTA, 1 mM DTT, 10% sucrose, 1 mM PMSF, leupeptin (0.2 mg/mL), aprotinin (0.2 mg/mL), and 100  $\mu\text{M}$  digitonin. Digitonin permeabilization is required to avoid artifacts due to the mechanical breakage of the outer mitochondrial membrane by dounce homogenization or ultrasonic disruption. Cell lysates were centrifuged at  $14,000\text{ g}$  for 20 min and the protein concentrations of the cytosolic supernatants were determined with the BCA Protein Assay Kit. For PARP-1 cleavage, aliquots of supernatants containing equal 100  $\mu\text{g}$  quantities of proteins were incubated with 6 M urea in SDS sample loading buffer for 15 min at  $65^{\circ}$ , resolved by electrophoresis for 1 hr at 175 V in a 10% SDS–polyacrylamide gel, and transferred for 1 hr to a PVDF sequencing membrane (Immobilon-P<sup>SQ</sup>; Millipore) using a Panther model HEP1 Semidry Electrobloater (Owl Separation Systems) [21]. For Cyt *c* release, aliquots of supernatants containing equal 100  $\mu\text{g}$  amounts of proteins were boiled for 5 min in SDS sample loading buffer, resolved by electrophoresis for 75 min at 110 V in a 15% SDS–polyacrylamide gel, and transferred for 1 hr to the above PVDF sequencing membrane. The blots were blocked with 5% nonfat dry milk in 20 mM Tris–HCl buffer, pH 7.4, with 0.9% NaCl (TBS),

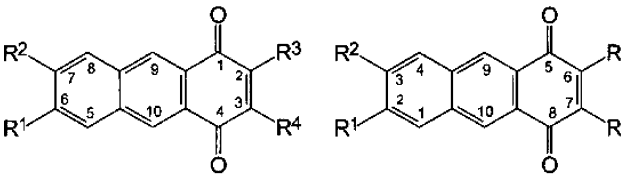


containing 0.05% of Tween-20 (TBST) for 2 hr at room temperature. Immunodetections of PARP-1 or Cyt *c* were conducted at room temperature overnight in TBST containing 2% of nonfat dry milk, using, respectively, 1 µg/mL mouse anti-PARP-1 (Ab-2) primary mAb (Oncogene), which recognizes both the 116-kDa native PARP-1 protein and its 85-kDa cleavage fragment [21], or 1 µg/mL of mouse anti-Cyt *c* (7H8.2C12) primary mAb (BD Pharmingen), which recognizes the 15-kDa denatured form of Cyt *c* [29]. After the blots were rinsed thrice with TBST, incubated for 1 hr at room temperature in TBST containing 2% of nonfat dry milk and goat anti-mouse secondary mAb conjugated with horseradish peroxidase (1:50,000 dilution; Oncogene), and rinsed again thrice with TBST, Kodak BioMax light film (Eastman Kodak) was used to develop images of the immunoreactive bands revealed by enhanced chemiluminescence staining, using the Super-Signal West Pico CL Substrate (Pierce). The integrated density values of Western blots were compared by digital image analysis (Chemi Imager 5500 with AlphaEase software), using a MultiImage Light Cabinet (Alpha Inotech Corp.).

### 3. Results

#### 3.1. Reduction of tumor cell proliferation and integrity by new AQ1 analogs

Since AQ1 and, to a lesser degree, its 6,7-dichloro derivative AQ4 are the most cytostatic AQ compounds synthesized so far [8,9], they have been selected as references to assess the effectiveness of the new compounds in the series. The chemical structures and code names of the six new AQ1 analogs synthesized to be tested for their antiproliferative activities in WT HL-60-S cells *in vitro* are shown in Fig. 1 and the correct nomenclatures of these compounds are as follows. AQ8: 6-methyl-1,4-anthracenedione. AQ9: 6-bromomethyl-1,4-anthracenedione. AQ10: 6-hydroxymethyl-1,4-anthracenedione. AQ11: 6-formyl-1,4-anthracenedione. AQ12: 2-bromo-6-methyl-1,4-anthracenedione and 2-bromo-7-methyl-1,4-anthracenedione. AQ13: 5,8-dioxo-5,8-dihydro-2-anthracenecarboxylic acid. AQ13 has no bioactivity whatsoever when tested up to 4 µM and AQ11 and AQ12 are less cytostatic than AQ4. But three new compounds, AQ10 and, especially, AQ8 and AQ9, are significantly more effective in the nanomolar range *in vitro* than AQ1 at reducing the growth of HL-60-S cells, based on the mitochondrial ability of these cells to metabolize the MTS:PMS reagent at day 4 (Fig. 1). Similar data are observed when comparing the losses of cellular integrity induced by 1.6 µM concentrations of these AQ1 analogs, using the Trypan blue exclusion test at 24 hr (Fig. 1) to rank the apoptotic potential of these drugs in the HL-60-S cell system [23,24]. Hence, AQ8 and AQ9 have been identified as new lead antiproliferative



Compound	Stained cells (%) at 24 h	IC <sub>50</sub> (nM) at day 4
AQ1 : R <sup>1</sup> = R <sup>2</sup> = R <sup>3</sup> = R <sup>4</sup> = H	21.9 ± 2.9	140 ± 7
AQ4 : R <sup>1</sup> = R <sup>2</sup> = Cl, R <sup>3</sup> = R <sup>4</sup> = H	7.1 ± 0.2	243 ± 16 <sup>a</sup>
AQ8 : R <sup>1</sup> = CH <sub>3</sub> , R <sup>2</sup> = R <sup>3</sup> = R <sup>4</sup> = H	36.4 ± 3.1	87 ± 4 <sup>b</sup>
AQ9 : R <sup>1</sup> = CH <sub>2</sub> Br, R <sup>2</sup> = R <sup>3</sup> = R <sup>4</sup> = H	42.7 ± 3.3	79 ± 3
AQ10: R <sup>1</sup> = CH <sub>2</sub> OH, R <sup>2</sup> = R <sup>3</sup> = R <sup>4</sup> = H	23.4 ± 3.2	125 ± 7 <sup>c</sup>
AQ11: R <sup>1</sup> = CHO, R <sup>2</sup> = R <sup>3</sup> = R <sup>4</sup> = H	1.5 ± 0.1	1,260 ± 104 <sup>d</sup>
AQ12: R <sup>1</sup> = CH <sub>3</sub> , R <sup>3</sup> = Br, R <sup>2</sup> = R <sup>4</sup> = H and R <sup>2</sup> = CH <sub>3</sub> , R <sup>3</sup> = Br, R <sup>1</sup> = R <sup>4</sup> = H	6.4 ± 0.4	327 ± 29 <sup>e</sup>
AQ13: R <sup>1</sup> = CO <sub>2</sub> H, R <sup>2</sup> = R <sup>3</sup> = R <sup>4</sup> = H	0.2 ± 0.1	NS <sup>f</sup>

Fig. 1. Structures, code names, % of stained cells at 24 hr, and concentrations of AQ1 analogs required to inhibit by 50% the metabolic activity of human HL-60-S cells at day 4 *in vitro*. The losses of cellular integrity (means ± SD, N = 3) were compared by the Trypan blue exclusion test 24 hr after treatment with 1.6 µM concentrations of the indicated compounds. The background level of stained cells (4.5 ± 0.4%) in untreated control incubates was subtracted from the results. Cell proliferation results (means ± SD, N = 3) were expressed as % of the net absorbance of MTS/formazan after bioreduction by vehicle-treated control tumor cells ( $A_{490\text{ nm}} = 1.627 \pm 0.081$ , 100 ± 5%) after 4 days in culture. The blank value ( $A_{490\text{ nm}} = 0.315$ ) for cell-free culture medium supplemented at day 4 with MTS:PMS reagent was subtracted from the results. IC<sub>50</sub> values were calculated from linear regression of the slopes of the log-transformed concentration–survival curves. <sup>a</sup> $P < 0.005$ , greater than AQ1; <sup>b</sup> $P < 0.05$ , greater than AQ9 but  $P < 0.005$ , smaller than AQ10; <sup>c</sup> $P < 0.05$ , smaller than AQ1; <sup>d</sup> $P < 0.0005$ , greater than AQ12; <sup>e</sup> $P < 0.025$ , greater than AQ4; <sup>f</sup> not significantly different from control when tested up to 4 µM.

compounds to study the mechanism of AQ-induced apoptosis in HL-60 tumor cells.

#### 3.2. Induction of DNA fragmentation by AQ8 and AQ9

The abilities of AQ8 and AQ9 to induce internucleosomal DNA fragmentation at 24 hr have been demonstrated by two different techniques, using HL-60-S cells containing [<sup>3</sup>H]thymidine-prelabeled DNA to detect low molecular weight DNA fragments after intact chromatin precipitation (Fig. 2) or agarose gel electrophoresis to visualize the typical pattern of DNA laddering indicative of apoptosis (Fig. 3). As reported before for AQ1 in L1210 and HL-60 cells [8,9], the concentration-dependent inductions of DNA cleavage caused by AQ8 and AQ9 in HL-60-S cells at 24 hr are similarly biphasic, starting at 256 nM, peaking 49–66% above control level (5.9% DNA fragmentation) at 4 µM, but then declining toward or even below the control % of DNA fragmentation at higher 10–25 µM concentrations (Fig. 2). The same biphasic increase and decrease of internucleosomal DNA fragmentation is verified by agarose gel electrophoresis of DNA samples extracted after 24 hr from HL-60-S cells treated with increasing

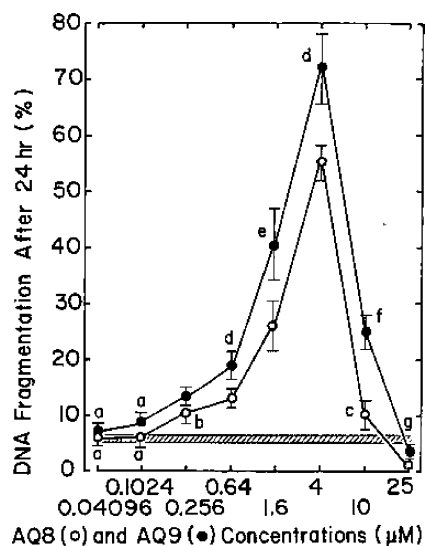


Fig. 2. Comparison of the concentration-dependent inductions of DNA fragmentation by AQ8 (○) and AQ9 (●) at 24 hr in HL-60-S cells containing  $^3\text{H}$ -prelabeled DNA *in vitro*. Results are expressed as [cpm in supernatant/cpm in supernatant + pellet]  $\times 100$  at 24 hr. For untreated control tumor cells ( $5.9 \pm 0.6\%$  DNA fragmentation, striped area), the supernatant (DNA fragments) is  $3,899 \pm 378$  cpm and the pellet (intact DNA) is  $62,225 \pm 6,496$  cpm. Bars: means  $\pm$  SD ( $N = 3$ ). <sup>a</sup>Not different from control; <sup>b</sup> $P < 0.025$  and <sup>c</sup> $P < 0.05$ , greater than control; <sup>d</sup> $P < 0.025$ , <sup>e</sup> $P < 0.05$ , and <sup>f</sup> $P < 0.005$ , greater than similar concentrations of AQ8; <sup>g</sup> $P < 0.025$ , smaller than control.

concentrations of AQ8 and AQ9 (Fig. 3). As compared to controls, DNA cleavage bands with a characteristic pattern of internucleosomal ladders become increasingly visible in response to 41–640 nM concentrations of these drugs, peak at 1.6–4  $\mu\text{M}$  AQ8 and AQ9, and then almost disappear in response to 10–25  $\mu\text{M}$  AQ8 and AQ9, presumably because the higher concentrations of these cytostatic drugs block the molecular events required to sustain the active process of apoptotic DNA fragmentation (Fig. 3).

### 3.3. Induction of PARP-1 cleavage by new AQ1 analogs

A time-dependent induction of PARP-1 cleavage is observed in HL-60-S cells treated with the lead antiproliferative AQ9 (Fig. 4, top). There is no PARP-1 cleavage in untreated control but the band of the 85-kDa fragment becomes increasingly apparent 3 hr after AQ9 treatment and, in contrast to necrotic cells which contain large amounts of uncleaved PARP-1 [30], virtually no intact PARP-1 is left after 6 hr in apoptotic HL-60-S cells treated with 1.6  $\mu\text{M}$  AQ9 (Fig. 4, top). Hence, the concentration-dependent effects of AQ9 were assessed at 6 hr, the first time at which this drug can fully induce PARP-1 cleavage and the disappearance of the 116-kDa band of native enzyme. At 6 hr, therefore, increasing concentrations of AQ9 induce PARP-1 cleavage in a concentration-dependent manner, with partial effects up to 0.64  $\mu\text{M}$  and maximal effects at 1.6–4  $\mu\text{M}$  (Fig. 4, middle). Moreover, the effectiveness of our synthetic AQ1 analogs as inducers of

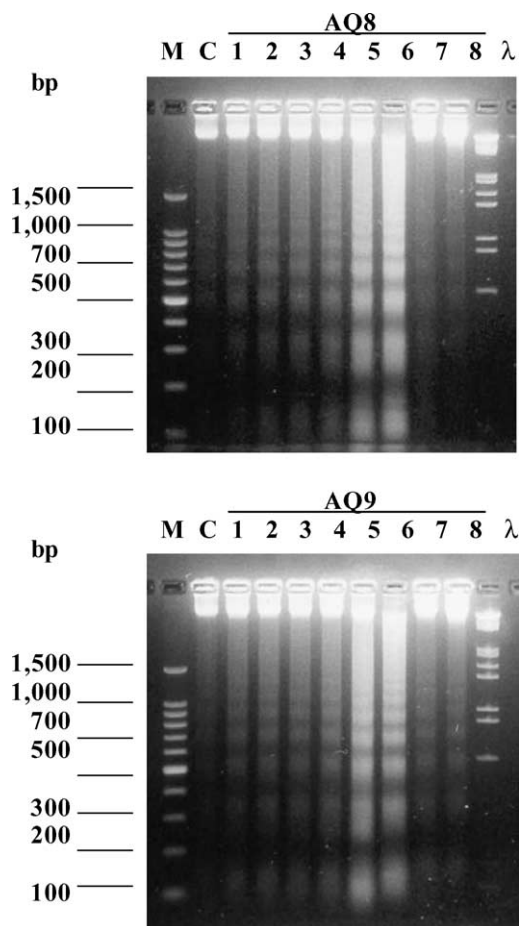


Fig. 3. Agarose gel analysis of drug-induced internucleosomal DNA fragmentation in HL-60-S cells *in vitro*. Concentration-dependent levels of DNA fragmentation in cells incubated at 37° for 24 hr in the presence or absence (control: lanes C) of 0.041, 0.102, 0.256, 0.64, 1.6, 4, 10, and 25  $\mu\text{M}$  AQ8 or AQ9 (lanes 1–8). Cellular DNA extracts (6  $\mu\text{g}/\text{well}$ ) were loaded onto a 1.5% agarose gel containing ethidium bromide (1  $\mu\text{g}/\text{mL}$ ), separated by electrophoresis for 3.7 hr at 60 V, and photographed under UV light. A typical ladder pattern indicating the presence of DNA equivalent to the size of single and oligo nucleosomes is characteristic of apoptosis. Size markers are shown in lanes M (0.5  $\mu\text{g}$  of 100 bp standard DNA ladder) and  $\lambda$  (0.75  $\mu\text{g}$  of lambda DNA/*EcoRI* + *HindIII* markers).

PARP-1 cleavage (Fig. 4, bottom) may be related to their ability to decrease tumor cell proliferation and integrity (Fig. 1). When compared at 4  $\mu\text{M}$ , full PARP-1 cleavage is induced by the most cytostatic compounds AQ1, AQ8, AQ9, and AQ10, as indicated by the nearly total disappearance of the 116-kDa band of native enzyme in HL-60-S cells at 6 hr (Fig. 4, bottom). In contrast, based on the intensity of the 116-kDa remnant and the smaller band of 85-kDa fragment, PARP-1 is certainly cleaved to a lesser degree by the less cytostatic compounds AQ4 and AQ12 (Fig. 4, bottom).

### 3.4. Activation of the caspases 9 and 3 cascade by new AQ1 analogs

Because the degradation of PARP-1 is catalyzed by caspase-3, the key downstream effector caspase which is

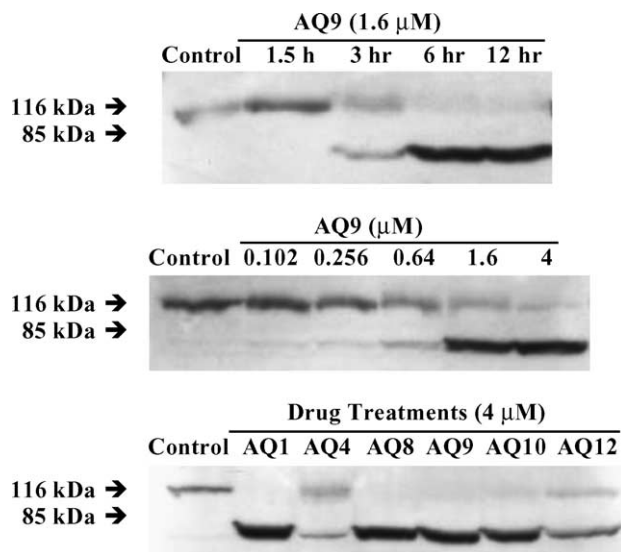


Fig. 4. Induction of PARP-1 cleavage by new AQ1 analogs in HL-60-S cells *in vitro*. Tumor cells were incubated for the indicated periods of time in the presence or absence (control) of various concentrations of drugs and bands (arrows) of intact ( $M_r \sim 116,000$ ) and cleaved ( $M_r \sim 85,000$ ) PARP-1 were detected by Western blot analysis. Top: time-dependent induction of PARP-1 cleavage by 1.6 μM AQ9. Middle: concentration-dependent induction of PARP-1 cleavage by AQ9 after 6 hr. Bottom: comparison of the abilities of 4 μM concentrations of lead antiproliferative AQ1 analogs to induce PARP-1 cleavage after 6 hr.

proteolytically activated by the initiator caspase-9, the AQ treatments shown to induce PARP-1 cleavage were tested for their ability to activate the postmitochondrial cascade of caspases 9 and 3. The hypothesis that caspase-3 is involved in PARP-1 cleavage at 6 hr is substantiated by the fact that there is a rapid induction of caspase-3 activity, which peaks at 313–380% of the control 6 hr after AQ8 and AQ9 treatments in HL-60-S cells (Fig. 5). But 1.6 μM AQ9 is more potent than 1.6 μM AQ8 and nearly matches the peak induction of caspase-3 activity caused by 4 μM AQ8, suggesting that AQ9 is a lead antiproliferative compound somewhat more effective than AQ8 at triggering apoptosis in HL-60-cells (Fig. 5). This observation is supported by the finding that caspase-9 and -3 activities are both maximally induced (between 412 and 577% of the controls) 6 hr after treatments with 1.6 μM AQ9 and 4 μM AQ8 in HL-60-S cells (Fig. 6, top). Interestingly, the concentration-dependent abilities of AQ9 and AQ8 to maximally induce caspase-9 and -3 activities in HL-60-S cells at 6 hr are similarly biphasic and resemble the biphasic inductions of internucleosomal DNA fragmentation caused by these drugs at 24 hr (Figs. 2 and 3), with the activations of caspases 9 and 3 increasing up to peaks at 1.6–4 μM followed by declines toward or even below the control levels for higher concentrations of AQ9 and AQ8, which presumably block the active process of apoptosis (Fig. 6, top). Moreover, 1.6 μM AQ9 and 4 μM AQ8 retain their ability to maximally induce, and in the same biphasic concentration-dependent manner as in the WT parental cells, caspase-9 and -3 activities (between 485 and 762% of

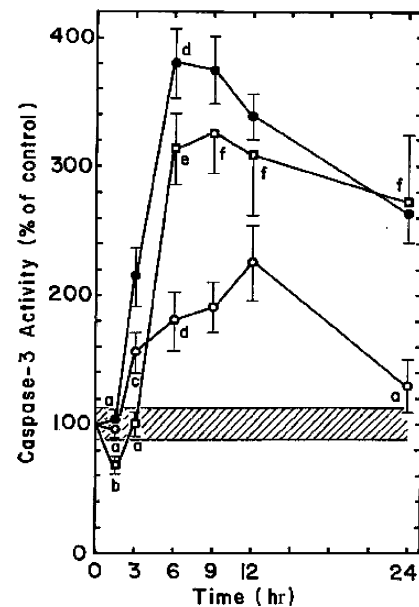


Fig. 5. Comparison of the time-dependent inductions of caspase-3-like protease activity by 1.6 (○) and 4 μM (●) concentrations of AQ8 and 1.6 μM AQ9 (□) in HL-60-S cells *in vitro*. Results are expressed as % of DEVD cleavage activity in vehicle-treated control tumor cells ( $14.9 \pm 1.8$  nM AFC released/mg protein,  $100 \pm 12\%$ , striped area) at each time point tested. Bars: means  $\pm$  SD (N = 3). <sup>a</sup>Not different from control; <sup>b</sup> $P < 0.025$ , smaller than control; <sup>c</sup> $P < 0.01$ , greater than control; <sup>d</sup>not different from the effects of similar treatments at 9 and 12 hr; <sup>e</sup>not different from the effects of similar treatments at 9, 12, and 24 hr but  $P < 0.01$ , smaller than the effect of 4 μM AQ8 at 6 hr; <sup>f</sup>not different from the respective effects of 4 μM AQ8 at 9, 12, and 24 hr.

the controls) in the MDR HL-60-RV cells at 6 hr (Fig. 6, bottom), an absence of resistance factor which is consistent with the fact that AQ1 also retains its ability to induce internucleosomal DNA fragmentation in these MDR tumor cells at 24 hr [9]. The AQ1 analogs which reduce tumor cell proliferation and integrity to various degrees in Fig. 1 were compared for their ability to induce the apoptotic caspase cascade in Fig. 7. In contrast to the least cytostatic AQ11, which is active at 4 μM but is the sole compound unable to induce caspase-9 and -3 activities at 1.6 μM, all the other AQ1 analogs are active at 1.6 μM, AQ8 inducing caspase-9 and -3 activities consistently more than AQ1, AQ4, AQ10, and AQ12, with 1.6 μM AQ9 even nearly matching the caspase-inducing potency of 4 μM AQ8 (Fig. 7). And because the caspase-inducing activity of the most potent AQ9 peaks at 1.6 μM, it has already declined at 4 μM (Fig. 7). AQ4 could not be tested at 4 μM in Fig. 7 because a stock solution 500 times more concentrated of this compound was not soluble in DMSO. Finally, HL-60-S cells were exposed to AQ8 and AQ9 for only 1 hr before these drugs were removed and caspase-9 and -3 activities were assayed as usual at 6 hr (Fig. 8). Again, the caspase-inducing activity of AQ9 definitively peaks at 1.6 μM rather than 4 μM (Fig. 8). But these 1-hr pulse treatments with 4 μM AQ8 and 1.6–4 μM AQ9 are sufficient to trigger as much induction of caspase-9 and -3 activities at 6 hr as when the antiproliferative drugs are

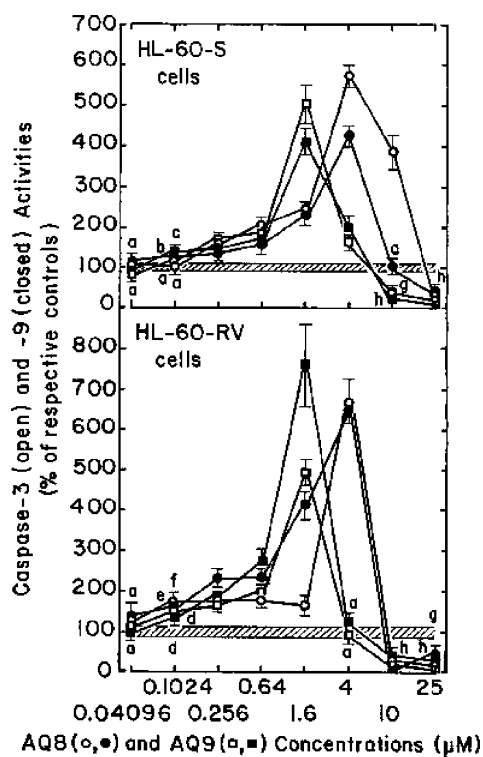


Fig. 6. Comparison of the concentration-dependent inductions of caspase-3-like (open symbols) and caspase-9-like (closed symbols) protease activities by AQ8 (circles) and AQ9 (squares) after 6 hr in HL-60-S (top) and HL-60-RV (bottom) cells *in vitro*. Results are respectively expressed as % of DEVD ( $13.3 \pm 1.1$  nmol AFC released/mg protein) or LEHD ( $4.5 \pm 0.4$  nmol AFC released/mg protein) cleavage activities in vehicle-treated control HL-60-S cells ( $100 \pm 8\%$ , striped area, top) and % of DEVD ( $8.6 \pm 0.9$  nmol AFC released/mg protein) or LEHD ( $2.5 \pm 0.3$  nmol AFC released/mg protein) cleavage activities in vehicle-treated control HL-60-RV cells at 6 hr ( $100 \pm 11\%$ , striped area, bottom). Bars: means  $\pm$  SD ( $N = 3$ ). <sup>a</sup>Not different from respective controls; <sup>b</sup> $P < 0.05$ , <sup>c</sup> $P < 0.025$ , <sup>d</sup> $P < 0.01$ , <sup>e</sup> $P < 0.005$ , and <sup>f</sup> $P < 0.0005$ , greater than respective controls; <sup>g</sup> $P < 0.005$  and <sup>h</sup> $P < 0.0005$ , smaller than respective controls.

maintained in the culture medium for the whole 6-hr period of incubation, suggesting that the mechanisms by which AQ1 analogs rapidly stimulate the apoptotic pathway are irreversible and persist after drug removal (Fig. 8).

### 3.5. Induction of Cyt *c* release by new AQ1 analogs

Because Cyt *c* release may be the limiting factor in caspase-9 activation and represents a central coordinating step in apoptosis [29,31], the AQ treatments shown to induce caspase-9 activity were tested for their ability to trigger Cyt *c* release in HL-60-S cells. The ability of 4  $\mu$ M AQ9 to induce the release of mitochondrial Cyt *c* into the cytosol of HL-60-S cells is time dependent (Fig. 9, top). As compared to untreated controls, the 15-kDa band of cytosolic Cyt *c* is increasingly visible at 1.5–3 hr and fully developed at 6 hr, a time which was then selected to determine the concentration dependency of this effect in Fig. 9 (middle). Under this condition, 0.102–0.64  $\mu$ M concentrations of AQ9 become increasingly effective at

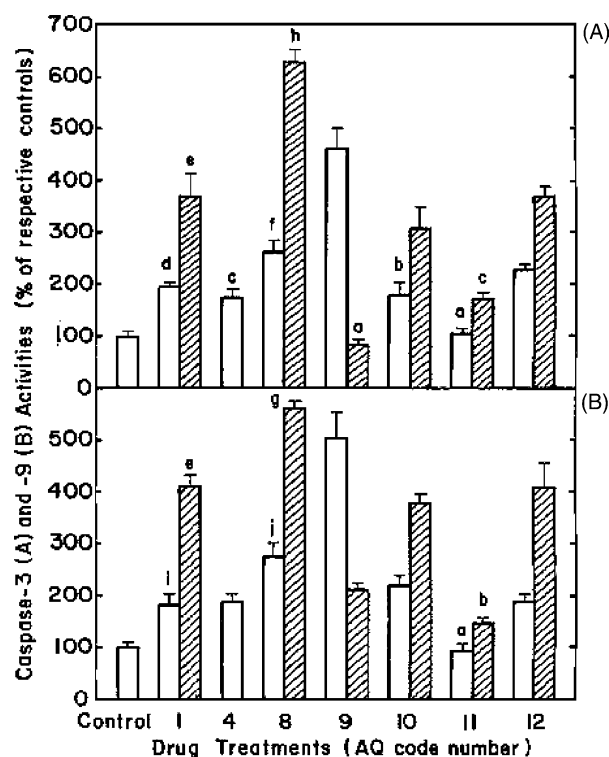


Fig. 7. Comparison of the abilities of 1.6  $\mu$ M (open) and 4  $\mu$ M (striped) concentrations of lead antiproliferative AQ analogs to induce caspases 3- (A) and 9-like (B) protease activities after 6 hr in HL-60-S cells *in vitro*. Results are, respectively, expressed as % of DEVD ( $11.0 \pm 1.1$  nmol AFC released/mg protein,  $100 \pm 10\%$ , control in A) or LEHD ( $6.0 \pm 0.8$  nmol AFC released/mg protein,  $100 \pm 13\%$ , control in B) cleavage activities in vehicle-treated control tumor cells at 6 hr. Bars: means  $\pm$  SD ( $N = 3$ ). <sup>a</sup>Not different from respective controls; <sup>b</sup> $P < 0.01$  and <sup>c</sup> $P < 0.005$ , greater than respective controls; <sup>d</sup>not different from 1.6  $\mu$ M AQ4 and AQ10 but  $P < 0.01$ , smaller than 1.6  $\mu$ M AQ12; <sup>e</sup>not different from 4  $\mu$ M AQ10 and AQ12; <sup>f</sup> $P < 0.05$ , greater than 1.6  $\mu$ M AQ12 but  $P < 0.005$ , smaller than 1.6  $\mu$ M AQ9; <sup>g</sup> $P < 0.01$  and <sup>h</sup> $P < 0.0005$ , greater than 4  $\mu$ M AQ12; <sup>i</sup> $P < 0.01$ , greater than control but not different from 1.6  $\mu$ M AQ4, AQ10, and AQ12; <sup>j</sup> $P < 0.05$ , greater than 1.6  $\mu$ M AQ10 but  $P < 0.005$ , smaller than 1.6  $\mu$ M AQ9.

triggering the release of Cyt *c*, which is maximally stimulated in response to 1.6–4  $\mu$ M AQ9 (Fig. 9, middle). When compared at 4  $\mu$ M, all cytostatic AQ1 analogs produce dense 15-kDa bands of Cyt *c* extracted from the cytosol of HL-60-S cells at 6 hr but, with the exception of the somewhat weaker AQ4, this concentration may be too high to determine whether the magnitudes of their Cyt *c* responses correlate to their antiproliferative activities (Fig. 9, bottom).

### 3.6. Role of initiator caspases 2 and 8 in AQ8- and AQ9-induced apoptosis

Since caspase-2 and -8 activities may act upstream of mitochondria to promote Cyt *c* release and the activation of the postmitochondrial initiator caspase-9, it is of interest to show that a treatment with 1.6  $\mu$ M AQ9 can induce all three initiator caspase-2, -8 and -9 activities tested in a time-dependent manner in HL-60-S cells (Fig. 10). But caspase-2 activity already peaks at 6 hr, whereas caspase-8



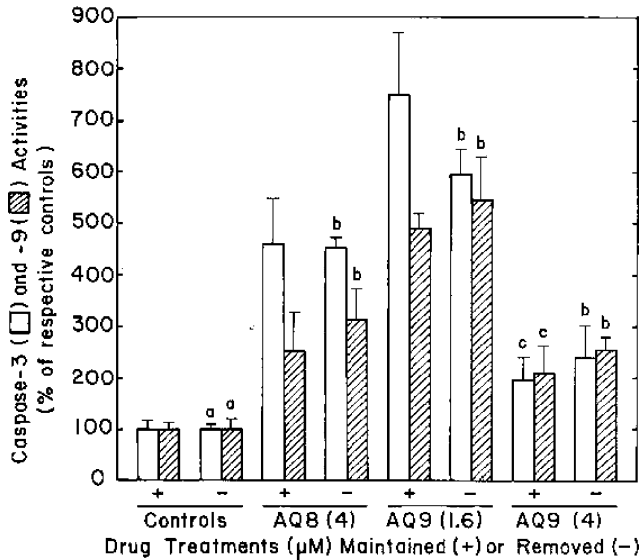


Fig. 8. Irreversibility of the abilities of 4  $\mu$ M AQ8 and 1.6 and 4  $\mu$ M concentrations of AQ9 to induce caspases 3- (open) and 9-like (striped) protease activities after 6 hr in HL-60-S cells *in vitro*. The drugs were either maintained in the medium for the whole 6-hr period of incubation (+) or removed after the first hour (-) in order to complete the remaining 5 hr of incubation in the absence of drugs. Results are respectively expressed as % of DEVD ( $12.0 \pm 2.0$  nmol AFC released/mg protein,  $100 \pm 17\%$ , open control, +) and LEHD ( $4.5 \pm 0.5$  nmol AFC released/mg protein,  $100 \pm 11\%$ , striped control, +) cleavage activities in vehicle-treated control tumor cells similarly incubated for 6 hr or % of DEVD ( $14.5 \pm 1.4$  nmol AFC released/mg protein,  $100 \pm 10\%$ , open control, -) and LEHD ( $4.2 \pm 0.8$  nmol AFC released/mg protein,  $100 \pm 19\%$ , striped control, -) cleavage activities in untreated controls spun, washed, and resuspended in fresh medium after the 1st of the 6 hr of incubation. Bars: means  $\pm$  SD (N = 3). <sup>a</sup>Not different from respective controls, +; <sup>b</sup>not different from the respective effects of similar concentrations of drugs maintained, +; <sup>c</sup> $P < 0.0025$ , greater than respective controls, +.

and -9 activities, which are only partially stimulated at this time, need 9 hr to be fully induced by 1.6  $\mu$ M AQ9. Such different rates of initiator caspase activation might suggest that AQ9 sequentially induces caspase-2 before caspase-9 and -8 (Fig. 10). Indeed, preincubation with the specific caspase-2 inhibitor z-VDVAD-fmk (15  $\mu$ M) totally abolishes the ability of 4  $\mu$ M AQ8 to induce caspase-9, -3, and -8 activities (Fig. 11, bottom) in HL-60-S cells at 6 hr. In contrast, preincubation with the caspase-8 inhibitor z-IETD-fmk (15  $\mu$ M) fails to alter the caspase-2-, -9-, and -3-inducing activities of 4  $\mu$ M AQ8 (Fig. 11, bottom). However, the same caspase-2 and -8 inhibitors tested at 15, 25, 50  $\mu$ M (data not shown) and even 100  $\mu$ M are both unable to significantly alter the abilities of 1.6 and 4  $\mu$ M concentrations of AQ8 to induce the release of Cyt c from mitochondria at 6 hr (Fig. 11, top), indicating that caspase-2 and -8 activations are not absolutely required for Cyt c release during AQ1 analog treatment. Taken together, the results of Fig. 11 suggest that initial activation of apical caspase-2 is critical to mediate the apoptotic pathway by which cytostatic AQ1 analogs activate the postmitochondrial caspases 9 and 3 cascade and the mitochondrial amplification loop involving caspase-8. But micromolar

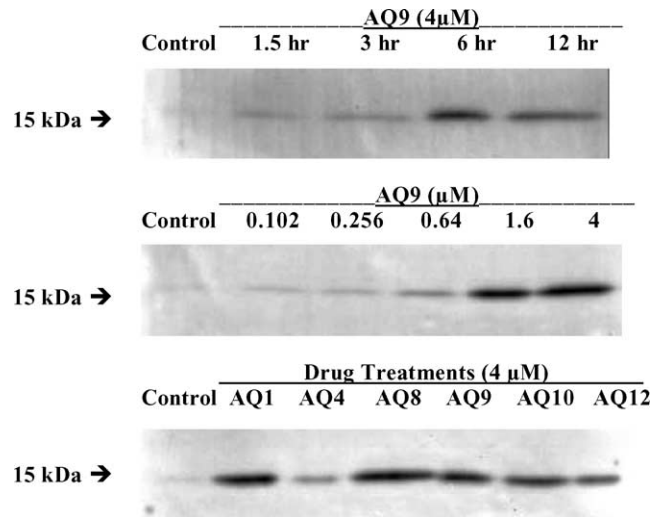


Fig. 9. Induction of Cyt c release by new AQ1 analogs in HL-60-S cells *in vitro*. Tumor cells were incubated for the indicated periods of time in the presence or absence (control) of various concentrations of drugs and bands (arrows) of cytosolic Cyt c ( $M_r \sim 15,000$ ) released from the mitochondrial intermembrane space were detected by Western blot analysis. Top: time-dependent induction of Cyt c release by 4  $\mu$ M AQ9. Middle: concentration-dependent induction of Cyt c release by AQ9 after 6 hr. Bottom: comparison of the abilities of 4  $\mu$ M concentrations of lead antiproliferative AQ1 analogs to induce Cyt c release after 6 hr.

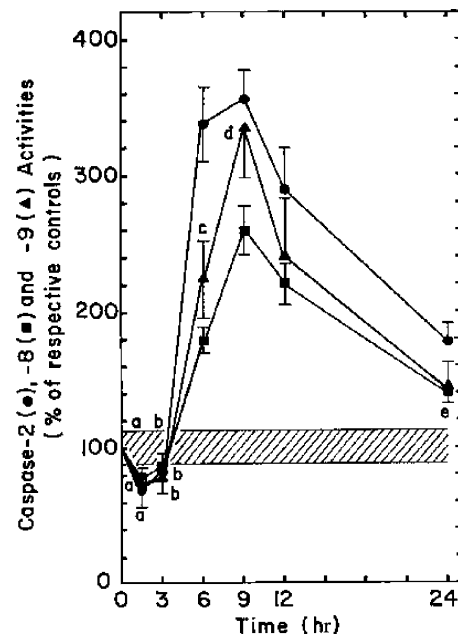


Fig. 10. Comparison of the time-dependent inductions of caspases 2- (●), 8- (■), and 9-like (▲) protease activities by 1.6  $\mu$ M AQ9 in HL-60-S cells *in vitro*. Results are respectively expressed as % of VDVAD ( $17.4 \pm 2.1$  nmol AFC released/mg protein), IETD ( $4.1 \pm 0.5$  nmol AFC released/mg protein), or LEHD ( $8.5 \pm 1.0$  nmol AFC released/mg protein) cleavage activities in vehicle-treated control tumor cells ( $100 \pm 12\%$ , striped area) at each time point tested. Bars: means  $\pm$  SD (N = 3). <sup>a</sup> $P < 0.05$ , smaller than controls; <sup>b</sup>not different from control; <sup>c</sup> $P < 0.05$ , greater than caspase-8 activity but  $P < 0.01$ , smaller than caspase-2 activity; <sup>d</sup>not different from caspase-2 activity but  $P < 0.05$ , greater than caspase-8 activity; <sup>e</sup> $P < 0.01$ , greater than control, not different from caspase-9 activity but  $P < 0.025$ , smaller than caspase-2 activity.

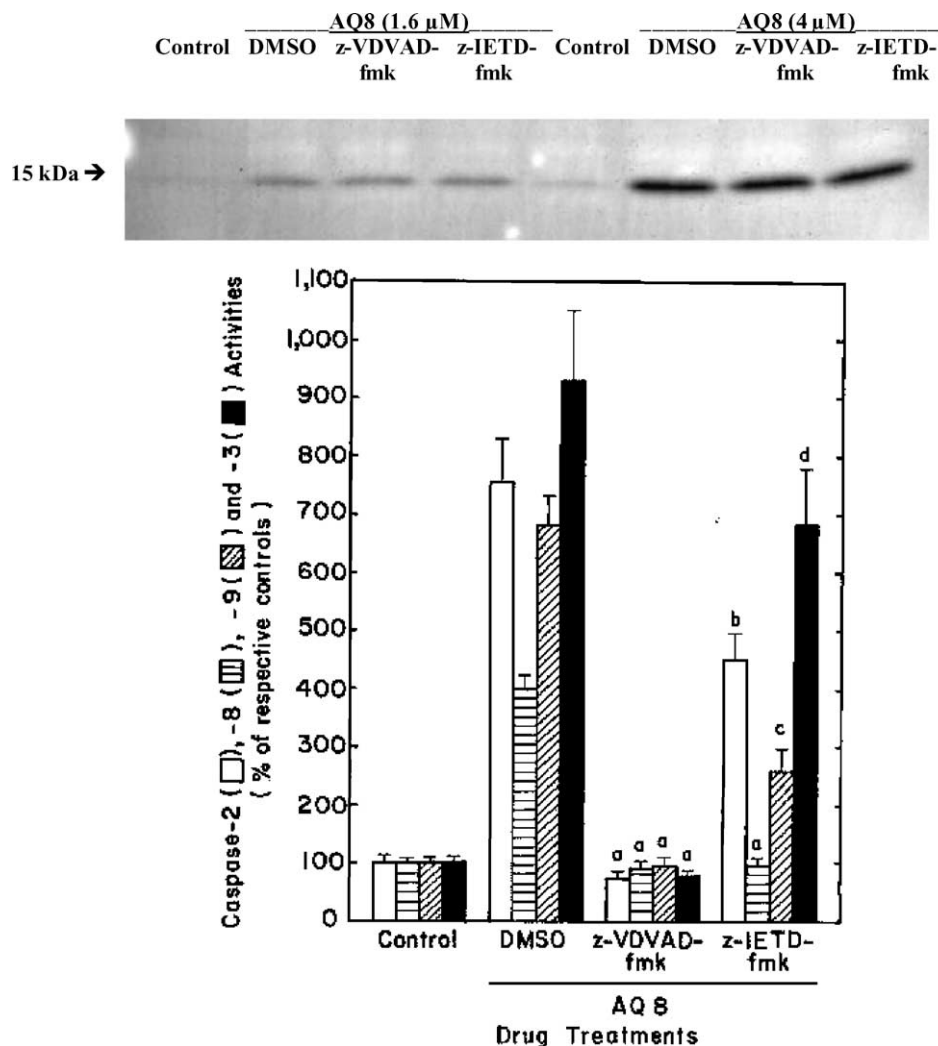


Fig. 11. Comparison of the abilities of caspase-2 and -8 inhibitors to prevent AQ8-induced Cyt *c* release (top) and initiator and effector caspase activities (bottom) in HL-60-S cells *in vitro*. Tumor cells were preincubated for 1 hr in the presence of vehicle, 15  $\mu$ M (bottom) or 100  $\mu$ M (top) concentrations of z-VDVAD-fmk or z-IETD-fmk and, after supplementing their culture medium with either vehicle (control) or 1.6  $\mu$ M (top) and 4  $\mu$ M (top and bottom) concentrations of AQ8, these incubations were continued for an additional 6 hr to determine Cyt *c* release and caspase-2-like activity or for an additional 8 hr to determine caspases 8-, 9-, and 3-like activities. Top: bands (arrow) of cytosolic Cyt *c* ( $M_r \sim 15,000$ ) released from the mitochondrial intermembrane space were detected by Western blot analysis. Bottom: caspases 2- (open), 8- (horizontal stripes), 9- (diagonal stripes), and 3-like (solid) activities are respectively expressed as % of VDAD ( $5.0 \pm 0.7$  nmol AFC released/mg protein), IETD ( $1.2 \pm 0.1$  nmol AFC released/mg protein), LEHD ( $2.6 \pm 0.2$  nmol AFC released/mg protein), or DEVD ( $9.2 \pm 0.9$  nmol AFC released/mg protein) cleavage activities in vehicle-treated control tumor cells. Bars: means  $\pm$  SD ( $N = 3$ ). <sup>a</sup>Not different from control; <sup>b</sup> $P < 0.005$ , smaller than AQ8; <sup>c</sup> $P < 0.0005$ , smaller than AQ8 but  $P < 0.005$ , greater than control; <sup>d</sup> $P < 0.05$ , smaller than AQ8.

concentrations of synthetic AQ1 analogs might also directly target mitochondria to trigger the release of Cyt *c* by a mechanism which appears to be independent from the premitochondrial action of apical caspases.

### 3.7. Role of the Fas/FasL signaling pathway in AQ9-induced apoptosis

Since AQ8 and AQ9 induce caspase-8 activity, antagonistic anti-Fas and anti-FasL mAbs have been used to determine whether Fas/FasL signaling is involved in the mechanism by which AQ1 analogs trigger apoptosis in HL-60-S cells (Fig. 12). The agonistic anti-Fas CH11 mAb induces Cyt *c* release and caspase-2, -8, and -9 activities

(302–485% of the controls) in HL-60-S cells at 6 hr and these effects are diminished (Fig. 12, top) or abolished (Fig. 12, bottom) by the antagonistic anti-Fas DX2 and ZB4 mAbs, which block the CD95 receptor, but not by the antagonistic anti-FasL NOK-1 mAb, which neutralizes the CD95 ligand (data not shown). The same pretreatments with blocking or neutralizing anti-Fas and anti-FasL clones, however, are totally unable to alter the ability of AQ9 to trigger Cyt *c* release (Fig. 12, top) and caspase-2, -8, and -9 activation in HL-60-S cells at 6 hr (Fig. 12, bottom), suggesting that the Fas/FasL pathway is neither involved in the mechanism of AQ-induced apoptosis nor even required for the induction of caspase-8 activity by the new AQ1 analogs. Densitometric analysis of Fig. 12 (top)

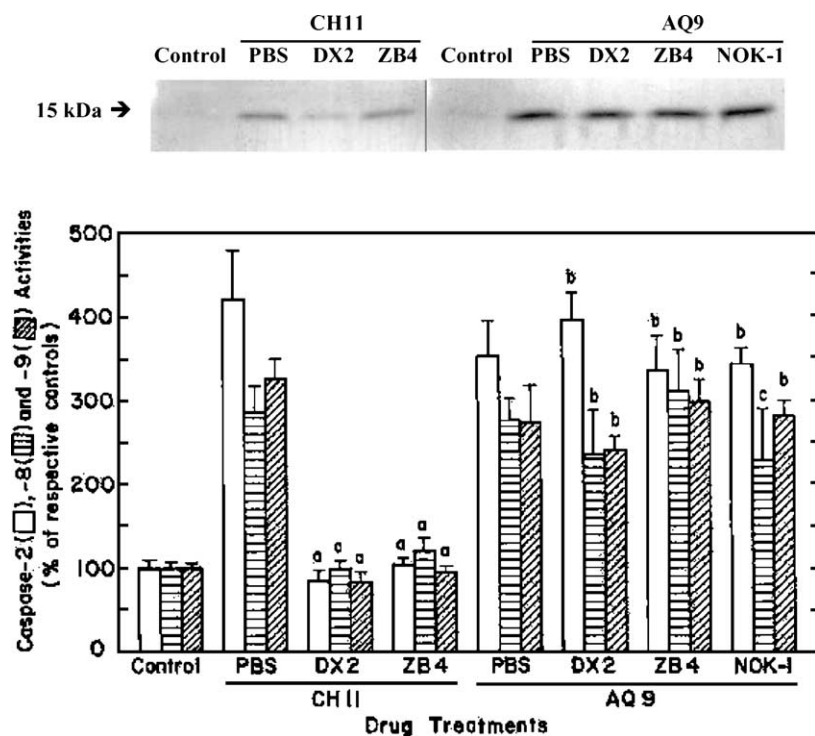


Fig. 12. Comparison of the abilities of antagonistic Fas and FasL mAbs to prevent the inductions of Cyt *c* release (top) and initiator caspase activities (bottom) by AQ9 and the agonistic CH11 mAb in HL-60-S cells *in vitro*. Tumor cells were preincubated for 1 hr in the presence of PBS, antagonistic anti-Fas DX2 and ZB4 mAbs (10  $\mu$ g/mL) or antagonistic anti-FasL NOK-1 mAb (10  $\mu$ g/mL) and, after supplementing their culture medium with either vehicle (control), 1.6  $\mu$ M AQ9, or agonistic anti-Fas CH11 mAb (1  $\mu$ g/mL), these incubations were continued for an additional 6 hr to determine Cyt *c* release and caspase-2-like activity or for an additional 7 hr to determine caspases 8- and 9-like activities. Top: bands (arrow) of cytosolic Cyt *c* ( $M_r \sim 15,000$ ) released from the mitochondrial intermembrane space were detected by Western blot analysis. Bottom: caspases 2- (open), 8- (horizontal stripes), and 9-like (diagonal stripes) activities are respectively expressed as % of VDAD ( $4.3 \pm 0.4$  nmol AFC released/mg protein), IETD ( $1.4 \pm 0.1$  nmol AFC released/mg protein), or LEHD ( $5.0 \pm 0.3$  nmol AFC released/mg protein) cleavage activities in vehicle-treated control tumor cells. Bars: means  $\pm$  SD ( $N = 3$ ). <sup>a</sup>Not different from respective controls; <sup>b</sup>not different from the respective effects of AQ9; <sup>c</sup> $P < 0.025$ , greater than control but not different from AQ9.

indicates that DX2 and ZB4, respectively, decrease CH11-induced Cyt *c* release by 53.4 and 22.5% without altering the Cyt *c* response to AQ9, which remains at 101–108% of its value.

#### 4. Discussion

Out of the 13 compounds tested so far, AQ8 and AQ9 are the lead antiproliferative drugs that are significantly more potent than the parental AQ1 structure from which they are derived. Based on its better  $IC_{50}$  value and ability to maximally induce early and late markers of apoptosis at 1.6  $\mu$ M rather than 4  $\mu$ M, AQ9 might be slightly more effective than AQ8. The cytostatic effects of AQ8 and AQ9 on leukemic cells *in vitro* are all the more remarkable that, among synthetic or naturally occurring quinones, the number of bioactive 1,2-, 1,4-, and 9,10-AQs appears quite limited, very few elicit antitumor effects *in vivo* and, with the exception of mitoxantrone, none of them seems to match the potency of our AQ1 analogs *in vitro* (reviewed in Ref. [9]). The 6,7-dichloro substitution of AQ4 does not improve, and the 2-(methylamino) addition tested earlier totally abolishes the antiproliferative activity of the AQ1

structure [9]. Because the equivalent 9,10-AQ compounds with their internal quinoid ring tested before are devoid of cytostatic activity [9], it is reasonable to assume that, substituted or not, the AQ1 framework with its external *para*-quinone is responsible for its potent antiproliferative activity in L1210 and HL-60 cells *in vitro*. Further structure–activity relationship (SAR) studies would be required to develop water-soluble AQ1 analogs that can be tested for their antitumor potential *in vivo*. Introduction of a methyl group at C6 increases the antiproliferative effect of AQ8 as compared to that of its parental AQ1 compound, an improvement which might be due to the increased lipophilicity provided by the alkyl group. Similarly, substitution of a bromomethyl group at C6 of AQ1 enhances even further the antiproliferative activity of AQ9, presumably because such bromomethyl group is an excellent electrophile that may undergo displacement reactions with various nucleophiles in the cells. Such AQ9 structure might elicit damaging effects in tumor cells through two reactive sites: the electrophilic bromomethyl substituent and the quinone moiety. Anthracenedione AQ10 possesses a C6 hydroxymethyl group and is slightly more potent than AQ1 but less active than AQ8, possibly because the hydroxyl group decreases the lipophilicity of the C6 substituent.

AQ12 is a mixture of 2-bromo-6-methyl- and 2-bromo-7-methyl-1,4-anthracenediones, two regioisomers that are inseparable by silica gel column chromatography. Since installation of a bromine onto C2 of AQ8 decreases the antiproliferative activity of AQ12, it is possible that the ability of AQ1 analogs to bind molecular targets in cells is hindered by the presence of a substituent on their quinone ring, a hypothesis supported by the fact that the 2-(methylamino) addition reported before also abolishes the bioactivities of the AQ1 and AQ4 structures [9]. AQ11, the 6-formyl derivative of AQ1 is the least effective cytostatic analog tested, perhaps because a hydrated form of AQ11 with lower lipophilicity than AQ1 may develop in the incubation medium (addition of a mole of water onto the aldehyde moiety). Its carboxylic acid function may also decrease the lipophilicity of AQ13 so much that this AQ1 analog becomes unable to reduce tumor cell proliferation and integrity even when tested at 4  $\mu$ M over a 4-day period.

In contrast to the early cleavage of DNA into large 50–300 kbp fragments, an initial signaling event that may induce tumor cells treated with relatively low concentrations of DNA-damaging anticancer drugs to commit apoptosis, the secondary endonucleolytic cleavage of DNA at internucleosomal linker sites to produce small 180–200 bp mono- and oligonucleosomal fragments at 24 hr is a late molecular marker concurrent with morphological evidence of apoptosis [19,32]. Upstream of DNA fragmentation, activation of the caspase cascade induces the proteolytic cleavage of a wide range of substrates. Effector caspase-3 activity cleaves and inactivates the inhibitor of caspase-activated DNase, thus releasing active endonuclease(s) that translocate into the nucleus to initiate internucleosomal DNA fragmentation [19,32]. The caspase-3-mediated cleavage and inactivation of PARP-1 is also an early critical event required for tumor cells that have been exposed to DNA-damaging anticancer drugs and have decided to commit apoptosis. PARP-1 cleavage may prevent the detection and repair of DNA damage, block the depletion of NAD<sup>+</sup> and ATP causing necrotic cell death, and enhance the activity of Ca<sup>2+</sup>/Mg<sup>2+</sup>-dependent endonucleases [30,33,34]. For this reason, detection of the disappearance of the native 116-kDa enzyme and appearance of the 85-kDa fragment of PARP-1 cleavage can serve as an early and sensitive indicator that AQ-treated cells are undergoing apoptosis [21]. The present study shows that, within 1 hr, certain AQ1 analogs rapidly trigger an irreversible apoptotic pathway that induces Cyt *c* release, postmitochondrial caspase activations and PARP-1 cleavage at 6 hr in relation with their ability to decrease tumor cell growth over a 4-day period, suggesting that the ability of these new quinone antiproliferative drugs to induce apoptosis may play a significant role in their molecular mechanism of action. The relatively low % of stained cells observed at 24 hr, using the Trypan blue exclusion test, suggests that 1.6  $\mu$ M concentrations of AQ1 analogs maximally induce within 6 hr an active process of apoptosis in cells which do not yet

have ruptured membranes. However, higher concentrations of AQ1 analogs may be cytotoxic *in vitro* since 100% of the HL-60 tumor cells treated for 24 hr with 50  $\mu$ M AQ1 are metabolically inert, have lost plasma membrane integrity, and are presumably dead (data not shown). Since the abilities of various AQ1 analogs to bind to nucleoside transporters, interact covalently with DNA, inhibit Topo activities, cause high molecular weight DNA strand breaks and crosslinks, induce MPT, block specific phases of cell cycle progression and affect the production of reactive O<sub>2</sub> species remain to be determined, it is rather premature to elaborate SARs, discuss potential primary molecular targets, and speculate on the nature of the initial and massive damaging events that within 1 hr induce AQ9-treated tumor cells to commit apoptosis. AQ1 analogs might trigger the different but sequentially related DNA-damaging events suggested to occur during etoposide (VP-16)-induced apoptosis. Rapid, massive, and unrepairable DNA damage secondary to Topo inhibition may be the trigger initiating nuclear signals that induce etoposide-treated tumor cells to release their mitochondrial Cyt *c* and undergo apoptosis, thereby activating their postmitochondrial caspase cascade responsible for PARP-1 cleavage, endonuclease activation and, ultimately, the internucleosomal fragmentation of their DNA, which is one of the late manifestations of the apoptotic process [32,35]. The basis for this hypothesis is that overexpressions of antiapoptotic bcl-2 or bcl-x<sub>L</sub>, which stabilize mitochondrial pores, abrogate Cyt *c* release and block the postmitochondrial caspase cascade, inhibit the later apoptotic events culminating in internucleosomal DNA fragmentation without affecting the early formation and repair of DNA single-strand breaks, double-strand breaks, and protein crosslinks caused by etoposide [35].

In the two major pathways of apoptosis, initiator caspase-8 is the first activated by death receptor signaling, whereas initiator caspase-9 is the first activated by cytotoxic chemotherapy and other genotoxic events [18,36]. Cytokines trigger the extrinsic pathway in which Fas receptor-mediated signals induce apical caspase-8 activation. The possible involvement of the Fas/FasL pathway in the apoptotic response of tumor cells to anticancer drugs is controversial. Even though some drug treatments may up-regulate the expression of the Fas/FasL system in certain cell lines, the Fas/FasL signaling pathway does not appear to be required to mediate the mechanism of anticancer drug-induced apoptosis [14,16,23,37–39]. Upon Fas cross-linking by the natural FasL or agonistic anti-Fas mAb, the receptor multimerization sequentially recruits the adaptor molecule Fas-associated death domain and procaspase-8, which bind to the receptor to form the death-inducing signaling complex where proteolytic activation of caspase-8 takes place. A large amount of activated caspase-8 may directly activate effector caspase-3 and the subsequent mitochondrial amplification loop involving the caspase-8-mediated cleavage of Bid [31]. Truncated Bid (tBid)



facilitates the insertion of Bax and Bak into the outer mitochondrial membrane where these proapoptotic bcl-2 family members trigger MPT and Cyt *c* release [40,41], which is the key limiting factor in initiating the postmitochondrial apoptotic protease cascade [31]. But a small amount of activated caspase-8 is sufficient to trigger Bid cleavage and mitochondrial Cyt *c* release and might be more efficient to amplify a signal otherwise too weak to directly induce caspase-3 activity and apoptosis [40–42]. DNA-damaging anticancer drugs trigger the mitochondrial-dependent intrinsic pathway in which nuclear-mediated signals likely to involve various p53-responsive genes directly induce the Bax- and Bak-mediated opening of the mitochondrial pores and the release of Cyt *c* [31]. After its release from the mitochondrial intermembrane space into the cytosol, Cyt *c* binds to apoptotic protease-activating factor-1 (Apaf-1), which through its caspase recruitment domain interacts with procaspase-9, resulting in the formation of the apoptosome complex that activates this initiator caspase in the presence of dATP [29,31]. In any case, all apoptotic pathways eventually converge on mitochondria and an activation of caspase-8 that does not require the death receptor but is mitochondrial-dependent may also play a role in chemotherapy-induced apoptosis. Hence, caspase-8 is involved in Fas-mediated apoptosis but may also be activated independently of Fas signaling and downstream of mitochondrial Cyt *c* release to mediate a secondary amplification loop, as suggested by the report that drug-induced caspase-8 activation does not require Fas/FasL interaction but is mitochondrial dependent [36]. Besides caspase-8 being activated after chemotherapy as a downstream event that follows caspase-9 activation, there is also evidence for the existence of a drug-inducible apoptotic pathway in which activation of caspase-8, and not caspase-9, forms the apical and mitochondrial-dependent step that subsequently activates the downstream caspases [36]. Among the apoptogenic factors released from mitochondrial interspace into the cytosol that can induce caspase-3 activity, Cyt *c* does not activate caspase-8 but apoptosis-inducing factor (AIF) does, suggesting that cleavage of procaspase-8 downstream of mitochondria requires AIF activity [43]. Even though nuclear and mitochondrial targets have not been studied yet, the present data suggest that cytostatic AQ1 analogs may trigger apoptosis in HL-60 cells by an intrinsic signaling pathway that does not involve the Fas/FasL system but is caspase-2 dependent. Positive controls using agonistic anti-Fas CH11 mAb to induce Cyt *c* release and caspase-2, -8, and -9 activities demonstrate that the cellular machinery required for the Fas signaling pathway is present, functional and responsive in the HL-60 tumor cell system. However, the antagonistic anti-Fas DX2 and ZB4 mAbs that reduce and abolish the proapoptotic effects of the CH11 clone and the antagonistic anti-FasL NOK-1 mAb that blocks the ligation of the natural FasL with its receptor are totally unable to prevent AQ9 from fully triggering the release of mitochondrial Cyt

*c* and the activation of the initiator caspases. Therefore, the fact that AQ9-induced apoptosis can proceed normally in the presence of various neutralizing and blocking agents that disrupt Fas/FasL interactions suggests that the Fas/FasL signaling pathway is not involved in this mechanism. Interestingly, the very same antagonistic anti-Fas and anti-FasL mAbs that block Fas-induced apoptosis also fail to inhibit DOX- and DAU-induced apoptosis in HL-60 and Jurkat tumor cells, suggesting that the signaling pathway by which these quinone antitumor drugs induce apoptosis is similarly Fas/FasL independent [14,16,23,44]. Moreover, our results indicate that both the Fas-mediated effects of CH11 and the Fas-independent effects of AQ9 on Cyt *c* release and initiator caspase activations in HL-60 cells are definitively p53-independent since p53 is not expressed in an active form in these p53-null HL-60 tumor cells [24,45].

Caspase-2 activity, which appears to be required for DNA damage-induced apoptosis and may be the first apical protease activated by the signals triggering AQ-induced apoptosis, may promote the translocation of proapoptotic Bax or tBid to mitochondria that results in the release of Cyt *c*, Smac, and AIF [46–48]. Based on their rates of activation, caspase-2 is maximally induced at 6 hr whereas caspase-9 and -8 activities peak at 9 hr, which may or may not indicate that caspase-2 precedes the other initiator caspases since submaximal activities of caspases 9 and 8 and maximal activity of caspase-3 are also detected at 6 hr. A more convincing argument is that, using a specific caspase-2 inhibitor, neither caspase-9, -3 nor -8 activations can occur in AQ8-treated HL-60 cells in the absence of caspase-2 activation, demonstrating that caspase-2 may be activated upstream of the other initiator and effector caspases and control their subsequent activations. Moreover, our results confirm that caspase-8 may be activated without Fas signaling after chemotherapy, an effect which is likely to occur in the postmitochondrial sequence since it is blocked in the absence of caspase-9 and -3 activations following caspase-2 inhibition. Because caspase-8 inhibition does not prevent AQ8 from activating caspases 2, 9, and 3, the activation of caspase-2 may be a key event required for the activation of the other downstream caspases and AQ-induced apoptosis can obviously proceed in the absence of caspase-8 activation, which may only play a secondary role as part of the mitochondrial amplification loop stimulated by the postmitochondrial caspase cascade. Hence, the concept that, in chemical-induced apoptosis, Cyt *c* release is caspase-independent may be true and is also observed in our study but the suggestion that caspase-9 is the 1st apical caspase activated [49] is not supported by this and other recent investigations [46–48], since caspase-2 inhibition does prevent caspase-9 activation. Caspase-2, which is located in the nucleus and may be the primary target of proapoptotic nuclear signals, has been postulated to be activated upstream of Cyt *c* release and caspase-9 activation in VP-16- and cisplatin-treated tumor cells [46–48]. So-called “low” and “high” concentrations of

VP-16 may trigger two distinct pathways for Cyt *c* release, 10  $\mu$ M inducing nuclear damage that signals the caspase-2-mediated release of mitochondrial Cyt *c* and 50  $\mu$ M directly disrupting mitochondria to induce MPT and Cyt *c* release [47,48]. The ability of AQ1 analogs to directly target mitochondria, induce MPT events and alter the ratio of bcl-2 family members controlling pore opening is under investigation but it should be noted that AQ9 fully induces Cyt *c* release, caspase-9 and -3 activations, PARP-1 cleavage, and internucleosomal DNA fragmentation in HL-60 cells at 1.6  $\mu$ M, suggesting that this drug may be a more potent inducer of apoptosis than VP-16. The different effects of z-VDVAD-fmk observed in Fig. 11 suggest that, whether or not caspase-2 acts upstream of mitochondria to induce some Cyt *c* release before activating the postmitochondrial cascade of caspases 9, 3, and 8, the activation of this apical caspase-2 is not absolutely required for AQ-induced Cyt *c* release, which can proceed in its absence. The non-essential role of apical caspases in mitochondrial Cyt *c* release is substantiated by the inability of 100  $\mu$ M of the caspase-8 inhibitor z-IETD-fmk to alter Cyt *c* release by 1.6–4  $\mu$ M AQ8. The conclusion is that caspase-2 may play an important role in mediating the mechanism of AQ-induced apoptosis but the critical release of mitochondrial Cyt *c* can occur independently from apical caspase activation during AQ1 analog treatments.

It should be noted that the  $IC_{50}$  value for the antiproliferative activity of AQ1 after 4 days of culture *in vitro* is much lower and closer to that of DAU in L1210 than in HL-60 cells, suggesting that its effectiveness may vary in different normal and tumor cell systems [8,9]. But the advantage of synthetic AQ1 analogs lies with the fact that, in contrast to DAU, these quinone antiproliferative drugs can also block nucleoside transport and retain their efficacy in HL-60 sublines that have developed different mechanisms of MDR [8,9]. Here, AQ8 and AQ9 induce caspase-9 and -3 activities as effectively in MDR HL-60-RV as in WT HL-60-S cells, a finding which is consistent with the report that AQ1 retains its ability to induce DNA fragmentation at 16–24 hr in these DAU-resistant tumor cells [9]. Apoptosis deficiency is strongly associated with the MDR phenotype. DOX induces Apaf-1 expression in WT p53 but not in p53 mutant cell lines. A lack of caspase-3-mediated PARP cleavage is observed in p53 mutant resistant to apoptosis and MDR HL-60 cells may lose surface Fas expression [23]. But AQ1 analogs and other quinone antitumor drugs can induce PARP-1 cleavage in p53-null HL-60-S and HL-60-RV cells [21] and, because the Fas pathway is not involved in AQ-mediated apoptosis in HL-60 cells, p53 deletion, and a deficiency in the activation of the Fas system suggested to play a role in MDR appear to be irrelevant to the apoptotic action of our antiproliferative AQ1 analogs. Recently, anticancer drugs including DOX have been shown to downregulate the mRNA levels of various inhibitor of apoptosis (IAP) proteins in WT but not in MDR HL-60 cells, suggesting that IAPs, which suppress

the activation of caspase-9 or directly bind to and inhibit the terminal caspases 3 and 7, may be involved in MDR [23]. Whether synthetic AQ1 analogs can circumvent the antiapoptotic activities of IAPs to activate caspases as effectively in MDR as in WT HL-60 cells remains to be investigated.

## Acknowledgments

This study was supported by grants from the National Institutes of Health (National Cancer Institute 5R01 CA86842-03 and Center of Biomedical Research Excellence 1P20 RR15563-03 with matching funds from the State of Kansas), the National Science Foundation (CHE-0078921 and REU-0097411), the American Heart Association, Heartland Affiliate (03506522), BioServe Space Technologies (NASA NAGW-1197), the Howard Hughes Medical Institute (Biological Sciences Education Grant), and Kansas State University (Terry C. Johnson Center for Basic Cancer Research). We thank Dr. Melvin S. Center, Kansas State University, Manhattan, KS, for providing us with the MDR HL-60-RV cell line.

## References

- [1] Marks TJ, Hanzlik RP, Cohen GM, Ross D, Graham DG. Quinone chemistry and toxicity. *Toxicol Appl Pharmacol* 1992;112:2–16.
- [2] Myers, CE, Chabner BA. Anthracyclines. In: Chabner BA, Collins JM, editors. *Cancer chemotherapy: principles and practice*. Philadelphia, PA: Lippincott; 1990. p. 356–81.
- [3] Rossi L, Moore GA, Orrenius S, O'Brien PJ. Quinone toxicity in hepatocytes without oxidative stress. *Arch Biochem Biophys* 1986; 251:25–35.
- [4] Qiu XB, Schönthal AH, Cadenas E. Anticancer quinone induce pRb-preventable G<sub>2</sub>/M cell cycle arrest and apoptosis. *Free Radic Biol Med* 1998;24:848–54.
- [5] Liu LF. DNA topoisomerase poisons as antitumor drugs. *Annu Rev Biochem* 1989;58:351–75.
- [6] Ling YH, Priebe W, Perez-Soler R. Apoptosis induced by anthracycline antibiotics in P388 parent and multidrug-resistant cells. *Cancer Res* 1993;53:1845–52.
- [7] Ramachandran C, You W, Krishan A. Bcl-2 and mdr-1 gene expression during doxorubicin-induced apoptosis in murine P388 and p388/R84 cells. *Anticancer Res* 1997;17:3369–76.
- [8] Perchellet EM, Magill MJ, Huang X, Dalke DM, Hua DH, Perchellet JP. 1,4-Anthraquinone: an anticancer drug that blocks nucleoside transport, inhibits macromolecule synthesis, induces DNA fragmentation, and decreases the growth and viability of L1210 leukemic cells in the same nanomolar range as daunorubicin *in vitro*. *Anticancer Drugs* 2000;11:339–52.
- [9] Wu M, Wang B, Perchellet EM, Sperfslage BJ, Stephany HA, Hua DH, Perchellet JP. Synthetic 1,4-anthracenediones, which block nucleoside transport and induce DNA fragmentation, retain their cytotoxicity in daunorubicin-resistant HL-60 cell lines. *Anticancer Drugs* 2001;12: 807–19.
- [10] Messner PW, Budihardjo II, Kaufman SH. Chemotherapy-induced apoptosis. *Adv Pharmacol* 1997;41:461–99.
- [11] Debatin KM. Activation of apoptosis pathways by anticancer treatment. *Toxicol Lett* 2000;112–113:41–8.

- [12] Kaufmann SH, Earnshaw WC. Induction of apoptosis by cancer chemotherapy. *Exp Cell Res* 2000;256:42–9.
- [13] Skladanowski A, Konopa J. Adriamycin and daunomycin induce programmed cell death (apoptosis) in tumour cells. *Biochem Pharmacol* 1993;46:375–82.
- [14] Gamen S, Anel A, Lasierra P, Alava MA, Martinez-Lorenzo MJ, Piñeiro A, Naval J. Doxorubicin-induced apoptosis in human T-cell leukaemia is mediated by caspase-3 activation in a Fas-independent way. *FEBS Lett* 1997;417:360–4.
- [15] Côme MG, Skladanowski A, Larsen AK, Laurent G. Dual mechanism of daunorubicin-induced cell death in sensitive and MDR-resistant HL-60 cells. *Br J Cancer* 1999;79:1090–7.
- [16] Ferraro C, Quemeneur L, Prigent AF, Taverne C, Pevillard JP, Bonnefoy-Berard N. Anthracyclines trigger apoptosis of both G<sub>0</sub>–G<sub>1</sub> and cycling peripheral blood lymphocytes and induce massive deletion of mature T and B cells. *Cancer Res* 2000;60:1901–7.
- [17] Hickman JA, Dive C, editors. Apoptosis and cancer chemotherapy. Totowa, NJ: Humana Press; 1999.
- [18] Budihardjo I, Oliver H, Lutter M, Luo X, Wang X. Biochemical pathways of caspase activation during apoptosis. *Annu Rev Cell Dev Biol* 1999;15:269–90.
- [19] Nagata S. Apoptotic DNA fragmentation. *Exp Cell Res* 2000;256:12–8.
- [20] Marquardt D, McCrone S, Center MS. Mechanisms of multidrug resistance in HL-60 cells: detection of resistance-associated proteins with antibodies against synthetic peptides that correspond to the deduced sequence of P-glycoprotein. *Cancer Res* 1990;50:1426–30.
- [21] Wang Y, Perchellet EM, Tamura M, Hua DH, Perchellet JP. Induction of poly(ADP-ribose) polymerase-1 cleavage by antitumor triptycene bisquinones in wild-type and daunorubicin-resistant HL-60 cell lines. *Cancer Lett* 2002;188:73–83.
- [22] Cory AH, Owen JC, Barltrop JA, Cory JG. Use of an aqueous soluble tetrazolium/formazan assay for cell growth assays in culture. *Cancer Commun* 1991;3:207–12.
- [23] Notarbartolo M, Cervello M, Dusanochet L, Cusimano A, D'Alessandro N. Resistance to diverse apoptotic triggers in multidrug resistant HL60 cells and its possible relationship to the expression of P-glycoprotein, Fas and of the novel anti-apoptosis factor IAP (inhibitory of apoptosis proteins). *Cancer Lett* 2002;180:91–101.
- [24] Kim SG, Ravi G, Hoffmann C, Jung YP, Kim M, Chen A, Jacobson KA. p53-independent induction of Fas and apoptosis in leukemic cells by an adenosine derivative, C1-IB-MECA. *Biochem Pharmacol* 2002;63:871–80.
- [25] Shi Z, Azuma A, Sampath D, Li YX, Huang P, Plunkett W. S-phase arrest by nucleoside analogues and abrogation of survival without cell cycle progression by 7-hydroxystaurosporine. *Cancer Res* 2001;61:1065–72.
- [26] Perchellet EM, Sperfslage BJ, Wang Y, Huang X, Tamura M, Hua DH, Perchellet JP. Among substituted 9,10-dihydro-9,10-[1,2]benzenoanthracene-1,4,5,8-tetraones, the lead antitumor triptycene bisquinone TT24 blocks nucleoside transport, induces apoptotic DNA fragmentation and decreases the viability of L1210 leukemic cells in the nanomolar range of daunorubicin *in vitro*. *Anticancer Drugs* 2002;13:567–81.
- [27] Miller SA, Dykes DD, Polesky HF. A simple salting out procedure for extracting DNA from human nucleated cells. *Nucleic Acids Res* 1988;16:1215.
- [28] Lai YL, Chen YJ, Wu TY, Wang SY, Chang KH, Chung CH, Chen ML. Induction of apoptosis in human leukemic U937 cells by tetrandrine. *Anticancer Drugs* 1998;9:77–81.
- [29] Liu X, Kim CN, Yang J, Jemmerson R, Wang X. Induction of apoptotic program in cell-free extracts: requirement for dATP and cytochrome c. *Cell* 1996;86:147–57.
- [30] Duriez PJ, Shah GM. Cleavage of poly(ADP-ribose) polymerase: a sensitive parameter to study cell death. *Biochem Cell Biol* 1997;75:337–49.
- [31] Li P, Nijhawan D, Budihardjo I, Srinivasula SM, Ahmad M, Alnemri ES, Wang X. Cytochrome c and dATP-dependent formation of Apaf-1/Caspase-9 complex initiates an apoptotic protease cascade. *Cell* 1997;91:479–89.
- [32] Compton MM. A biochemical hallmark of apoptosis: internucleosomal degradation of the genome. *Cancer Metastasis Rev* 1992;11:105–12.
- [33] Herceg Z, Wang ZQ. Functions of poly(ADP-ribose) polymerase (PARP) in DNA repair, genomic integrity and cell death. *Mutat Res* 2001;477:97–110.
- [34] Lazebnik YA, Kaufman SH, Desnoyers S, Poirier GG, Earnshaw WC. Cleavage of poly(ADP-ribose) polymerase by a proteinase with properties like ICE. *Nature* 1994;371:346–7.
- [35] Kamesaki S, Kamesaki H, Jorgensen TJ, Tanizawa A, Pommier Y, Cossman J. bcl-2 protein inhibits etoposide-induced apoptosis through its effects on events subsequent to topoisomerase II-induced DNA strand breaks and their repair. *Cancer Res* 1993;53:4251–6.
- [36] Ferreira CG, Span SW, Peters GJ, Krut FA, Giaccone G. Chemotherapy triggers apoptosis in a caspase-8-dependent and mitochondria-controlled manner in the non-small cell lung cancer cell line NCI-H460. *Cancer Res* 2000;60:7133–41.
- [37] Villunger A, Eggle A, Kos M, Hartmann BL, Geley S, Kofler R, Greil R. Drug-induced apoptosis is associated with enhanced Fas (APO-1/CD95) ligand expression but occurs independently of Fas (APO-1/CD95) signaling in human T-acute lymphatic leukaemia cells. *Cancer Res* 1997;57:3331–4.
- [38] McGahon AJ, Costa PA, Daly L, Cotter TG. Chemotherapeutic drug-induced apoptosis in human leukemic cells is independent of the Fas (APO-1/CD95) receptor/ligand system. *Br J Haematol* 1998;101:539–47.
- [39] Tolomeo M, Dusanochet I, Meli M, Grimaudo S, D'Alessandro N, Papoff G, Ruberti G, Rausa L. The CD95/CD95 ligand system is not the major effector in anticancer drug-mediated apoptosis. *Cell Death Differ* 1998;5:735–42.
- [40] Li H, Zhu H, Xu CJ, Yuan J. Cleavage of BID by caspase-8 mediates the mitochondrial damage in the Fas pathway of apoptosis. *Cell* 1998;94:491–501.
- [41] Scaffidi CA, Fulda S, Srinivasan A, Friesen C, Li F, Feng L, Tomaselli KJ, Debatin KM, Krammer PH, Peter ME. Two CD95 (APO-1/Fas) signaling pathways. *EMBO J* 1998;17:1675–87.
- [42] Kuwana T, Smith JJ, Muzio M, Dixit V, Newmeyer DD, Kornbluth S. Apoptosis induction by caspase-8 is amplified through the mitochondrial release of cytochrome c. *J Biol Chem* 1998;273:16589–94.
- [43] Fulda S, Scaffidi C, Susin SA, Krammer PH, Kroemer G, Peter ME, Debatin KM. Activation of mitochondria and release of mitochondrial apoptogenic factors by betulinic acid. *J Biol Chem* 1998;273:33942–8.
- [44] Lorenzo E, Ruiz-Ruiz C, Quesada AJ, Hernández G, Rodríguez A, López-Rivas A, Redondo JM. Doxorubicin induces apoptosis and CD95 gene expression in human primary endothelial cells through a p53-dependent mechanism. *J Biol Chem* 2002;277:10883–92.
- [45] Wolf D, Rotter V. Major deletions in the gene encoding the p53 tumor antigen cause lack of p53 expression in HL-60 cells. *Proc Natl Acad Sci USA* 1985;82:790–4.
- [46] Lässig P, Opitz-Araya X, Lazebnik Y. Requirement for caspase-2 in stress-induced apoptosis before mitochondrial permeabilization. *Science* 2002;297:1352–4.
- [47] Robertson JD, Gogvadze V, Zhivotovsky B, Orrenius S. Distinct pathways for stimulation of cytochrome c release. *J Biol Chem* 2000;275:32438–43.
- [48] Robertson JD, Enoksson M, Suomela M, Zhivotovsky B, Orrenius S. Caspase-2 acts upstream of mitochondria to promote cytochrome c release during etoposide-induced apoptosis. *J Biol Chem* 2002;277:29803–9.
- [49] Sien XM, MacFarlane M, Zhuang J, Wolf BB, Green DR, Cohen GM. Distinct caspase cascades are initiated in receptor-mediated and chemical-induced apoptosis. *J Biol Chem* 1999;274:5053–60.